Advances in Energy and Materials Research https://jaem.qom.ac.ir/

Exploring Structural and Interactional Properties of a Copper Complex: A Pathway to Energy Applications

Faeze Mojtabazade[✉1] and Zdirad Zák[2]

1. Corrsponding author, Department of Chemistry, Faculty of Sciences, Tarbiat Modares University, Tehran, Islamic Republic of Iran. Email: Faezeh.mojtabazadeh@modares.ac.ir
2. Department of Inorganic Chemistry, Faculty of Sciences, Masaryk University, Kotlárská 2, 611 37 Brno, Czech Republic. Email: zaak@chemi.muni.cz

Article Info

Article type:
Research Article

Article history:
Received 23 Jan 2024
Received in revised form 3 Mar 2024
Accepted 17 May 2024
Published online 24 Jun 2024

Keywords:
Copper Complex, π-π Interactions, Hydrogen Bonding, Hirshfeld surface analysis, Hydrogen bond.

ABSTRACT

This study presents the synthesis and characterization of a copper complex using a range of analytical techniques. The synthesized complex was confirmed via IR spectroscopy and further characterized by X-ray diffraction, which revealed a monoclinic crystal system with the Pī space group. Both internal and external hydrogen bonding interactions were observed. Notably, the complex exhibited significant π-π interactions between the phenyl rings of the L1 ligand's triazine ring and the adjacent triazine ring in the crystal lattice. Hirshfeld surface analysis highlighted that H···H interactions contributed over 50% to the overall surface interactions, with hydrogen bonding accounting for 13.6%. These findings provide valuable insights into the structural and interactional properties of copper complexes, which could pave the way for the development of novel materials with unique properties. Potential applications in catalysis, electronics, and medicine are discussed. This research not only enhances our understanding of copper complex interactions but also sets the stage for future studies exploring the synthesis of copper complexes with advanced functional properties.

Cite this article: Mojtabazade, F. & Zák, Z. (2024). Exploring Structural and Interactional Properties of a Copper Complex: A Pathway to Energy Applications, *Advances in Energy and Materials Research*, 1 (2), 1-6. https://doi.org/10.22091/jaem.2025.12059.1018

DOI: https://doi.org/10.22091/jaem.2025.12059.1018
Publisher: University of Qom.

1. Introduction

Copper compounds have been extensively studied due to their unique properties and potential applications in diverse fields, including medicine, electronics, and catalysis [1–7]. Copper complexes with acetate bridging have garnered considerable interest due to their intriguing structural properties [8–13]. The β-dicarbonyl motif is found in a variety of biologically and pharmaceutically active compounds [14–17] , and β-Diketones are particularly valuable in the treatment of various pathological conditions, including cardiovascular and liver diseases, hypertension, obesity, diabetes, neurological disorders, inflammation, skin diseases, and fibrosis[18,19]. The formation of these structures is of great interest to chemists due to their significant importance. Among the various complexes formed by β-diketones, copper β-diketones are particularly noteworthy [20,21]. In addition to their biological applications, including potent antibacterial properties [22], These compounds are widely used for extracting metals from water contaminated with heavy metals [23,24], and as catalysts [25]. Additionally, scientists have synthesized and studied copper β-diketone complexes to investigate the steric properties of β-diketone ligands. These studies offer valuable insights into the structural and electronic characteristics of these complexes [26].

2. Experimental

2.1. Synthesis

[Cu(L1)$_2$(pbdo)$_2$] (1): A solution was prepared by mixing 0.03 g (0.16 mmol) of L1, 0.06 g (0.32 mmol) of Hpbdo (1-phenylbutane-1,3-dione), and 0.01 g (0.04 mmol) of copper chloride salt in water. The mixture was then slowly transferred into a branched tube, and methanol was added gradually until the solution reached a level just above the side branch. The tube was sealed and placed in a paraffin bath at 60°C for four days. After this period, green crystals were formed, isolated, and washed with acetone and ether before being dried. The yield was 77%, with a melting point above 250°C. The calculated elemental composition for $C_{38}H_{36}CuN_{10}O_4$ was: C 60.03%, H 4.77%, N 18.42%, Cu 8.36%. The experimentally determined values were: C 60.75%, H 4.91%, N 18.23%, and Cu 8.58%.

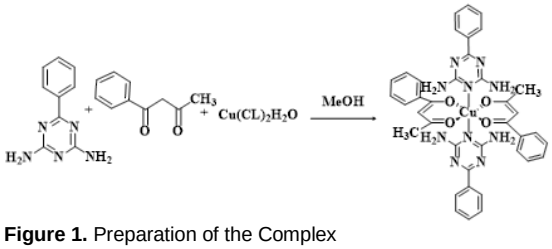

Figure 1. Preparation of the Complex

2.2. X-Ray Diffraction

Table 1 presents the crystallographic data for the complex, which were obtained through X-ray diffraction analysis.

Table 1. The Crystallographic Data

Empirical formula	$C_{19}H_{18}Cu_{0.50}N_5O_2$
Formula weight	380.15
Temperature/K	293(2)
Crystal system	Triclinic
Space group	P$\bar{1}$
a/Å	7.5243(6)
b/Å	11.2902(10)
c/Å	12.0791(11)
α/°	110.427(8)
β/°	97.232(7)
γ/°	105.978(8)
Volume/Å^3	895.96(13)
Z	2
ρ_{calc}mg/mm^3	0.25
m/mm^{-1}	1.409
F(000)	395
Crystal size/mm^3	0.4 mm × 0.3 mm × 0.1 mm
2Θ range for data collection	3.0408 to 27.5684°
Index ranges	-9 ≤ h ≤ 9, -13 ≤ k ≤ 13, -14 ≤ l ≤ 14
Reflections collected	7240
Independent reflections	3155[R(int) = 0.0190]
Data/restraints/parameters	3155/5/266
Goodness-of-fit on F^2	1.408
Final R indexes [I>=2σ (I)]	R_1 = 0.0335, wR_2 = 0.0770
Final R indexes [all data]	R_1 = 0.0508, wR_2 = 0.0818
Largest diff. peak/hole / e Å^{-3}	2.72/-0.80
Flack parameter	0.55(5)

Table 2 presents a summary of the specific bond lengths observed in both complex.

Table 2. Selective Bond Lengths

Cu—N11	2.630(4)	Cu12^i—N11^i	2.630(4)
Cu—O22^i	1.9273 (12)	C61—C71	1.377 (3)
Cu—O22	1.9273 (12)	C71—C81	1.367 (3)
Cu—O12	1.9442 (12)	C81—C91	1.378 (3)
Cu—O12^i	1.9442 (12)	O12—C92	1.269 (2)
N11—C11	1.339 (2)	O22—C72	1.284 (2)
C41—C51	1.386 (3)	C82—C92	1.394 (3)
C41—C91	1.390 (3)	C92—C102	1.505 (3)

The bond angles observed in the complex are presented in **Table 3.**

Table 3. Bond Angles [°]

O22^i—Cu—O22	180.00 (8)	C71—C61—C51	119.9 (2)
O22^i—Cu—O12	86.24 (5)	C81—C71—C61	120.4 (2)
O22—Cu—O12	93.76 (5)	C71—C81—C91	120.1 (2)

O22^{i}—Cu—O22	**180.00 (8)**	**C71—C61—C51**	**119.9 (2)**
O22^{i}—Cu—O12^{i}	93.76 (5)	C81—C91—C41	120.4 (2)
O22—Cu—O12^{i}	86.24 (5)	C92—O12—Cu	124.50 (12)
N51—C11—N31	116.95 (18)	C22—C32—C42	120.3 (2)
C91—C41—C31	120.64 (19)	C82—C92—C102	118.79 (18)
C41—C51—C61	120.0 (2)		
O22^{i}—Cu—O22	180.00 (8)	C71—C61—C51	119.9 (2)
O22^{i}—Cu—O12	86.24 (5)	C81—C71—C61	120.4 (2)

2.3. IR Spectroscopy

The IR spectrum of the complex, confirming its synthesis, is shown in **Figure 1. Table 4** provides a summary of the interpretation and peak positions of key functional groups within the complex.

Table 4. Frequencies of Important Groups

NH_2 (Stretching)	3396, 3345	C-H (Acetylacetone)	2854
C=N	1587	C-N	1380
C=C (Aromatic)	1540	C-H (Bending Aromatic)	777
C-H (Stretching Aromatic)	3056	NH_2 (Out-of-plane bending)	830
C-H (Aliphatic)	2920	NH_2 (Scissor-like bending)	1458
C=O	1614		
C-H (Aliphatic)	2922	OH(Methanol)	3418
C=C (Aromatic)	1559	C=O	1590
C-H (Stretching Aromatic)	3060	C-H (Bending Aromatic)	759

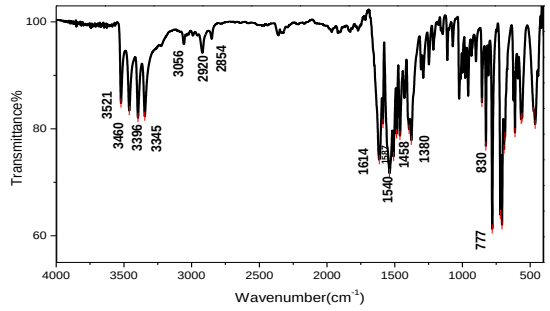

Figure 2. IR spectrum

2.4. Hirshfeld Analysis

The Crystal Explorer Ver. 3.1 program package was used to investigate the intermolecular interactions within the studied crystals. This analysis included Hirshfeld surface analysis, 2D fingerprint plots, and calculations of percentage contributions. Specifically, Hirshfeld surfaces were employed in this study, with no additional properties included in the calculation command.

3. Result and Discussion

The complex was synthesized by combining L1, Hpbdo, and copper chloride salt in a 1:8:4 ratio, using methanol as the solvent. X-ray diffraction analysis revealed that the complex crystallized in the triclinic crystal system with the Pī space group. Figure 2 illustrates that each copper atom is coordinated to two nitrogen atoms from two neutral 6-phenyl-1,3,5-triazine-2,4-diamine (L1) ligands, with a bond length of 2.630 (4) Å. Additionally, the copper atom is coordinated to four oxygen atoms from two monoanionic 1-phenylbutane-1,3-dione (Hpbdo) ligands, with bond lengths of 1.9442 (12) Å and 1.9273 (12) Å. This coordination results in a Cu^{2+} center with a trans-CuN_2O_4 coordination geometry. The compound exhibits a center of symmetry, allowing for the naming of only half of the molecule. The other half, with a symmetry code of -x, -y, -z, is obtained by reflecting the named part. The crystal network along the a- and b-axes is shown in **Figure 3.**

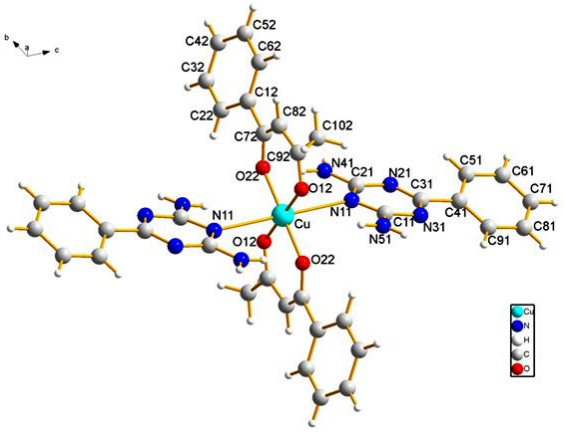

Figure 3. The Crystal Structure

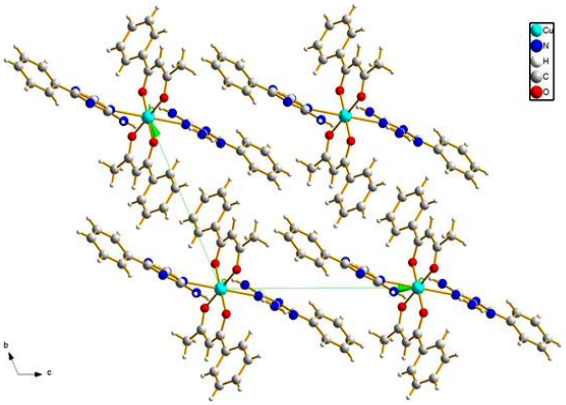

Figure 4. Crystal Network

In the crystal structure of the complex, the coordination sphere around each copper atom adopts an octahedral geometry. Two L1 ligands, coordinated through nitrogen atoms in the triazine ring, occupy the axial positions at the top and bottom, while two Hpbdo ligands, coordinated through oxygen atoms, occupy the equatorial positions (**Figure 4**). Additionally, the bond length between the L1 ligand and copper is longer than that between the Hpbdo ligand and copper. This disparity suggests a significant Jahn-Teller distortion along the direction of the L1 ligands. Jahn-Teller distortions are commonly observed in copper(II)

octahedral complexes due to their d^9 electron configuration.

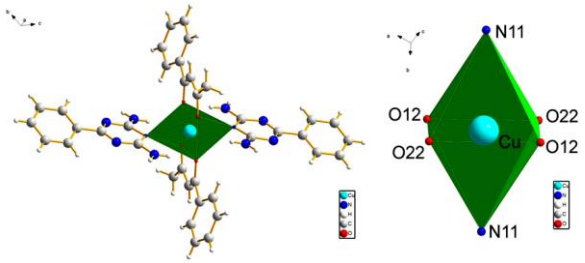

Figure 5. Coordination Sphere of Copper

This complex also exhibits hydrogen bonding, with details provided in Table 5. The crystal network of the complex contains various non-covalent interactions, including intramolecular and intermolecular hydrogen bonding, as well as π-π interactions. An intramolecular hydrogen bond is formed between the N-H groups of the L1 ligand and the coordinated oxygen atoms of the Hpbdo ligand. Intermolecular hydrogen bonds are established between the N-H groups of the L1 ligand and the oxygen atoms coordinated to the metal in the Hpbdo ligand of adjacent molecules.

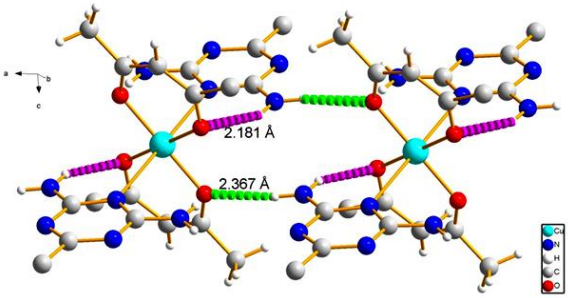

Figure 6. Hydrogen bonds

Table 5. Hydrogen Bond Information

D–H···A	D–H	H···A	D-A	D-H...A
O-H··· O22	0.87	2.147	2.889	134.40

In order to gain a deeper understanding of these interactions, we present the results of the Hirshfeld Surface Analysis. The Hirshfeld surfaces for the complexes are shown in Figure 5. This analysis employs the dnorm property to highlight specific regions of the surface. Blue regions indicate that the contact distance between atoms inside and outside the surface is greater than the sum of their respective van der Waals radii. White areas represent contact distances equal to the sum of the van der Waals radii, while small red regions indicate a contact distance that is less than the sum of the van der Waals radii.[28].

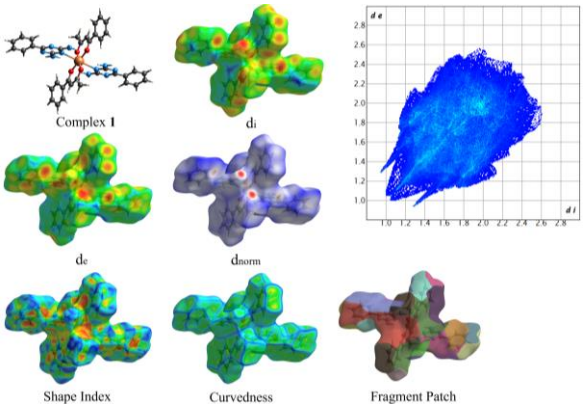

Figure 6. Hirshfeld surfaces analysis

Figure 6 provides a detailed breakdown of the percentage contributions by atoms to the surface area, offering deeper insights into the various interaction contributions within the complex. It is important to note that the calculations are based on reciprocal contacts, and thus internal and external terms are not included. H···H interactions make a significant contribution, accounting for 53.3% of the surface area in the complex. The total hydrogen bond contribution is 13.6%, while hydrogen-carbon interactions also play a notable role, contributing 25.8% to the surface.

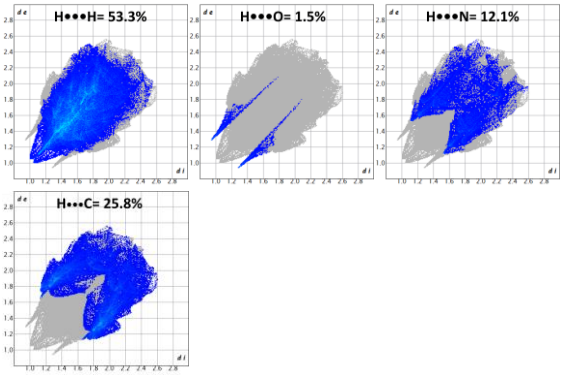

Figure 7. Surface Contributions Percentage

4. Conclusion

In conclusion, this research successfully synthesized a copper complex and confirmed its structure through IR spectroscopy. The complex was further characterized using X-ray diffraction, which revealed that $[Cu(L1)_2(pbdo)_2]$ crystallized with an octahedral coordination sphere in the triclinic crystal system, adopting the Pī space group. The complex exhibits both internal and external hydrogen bonding. Additionally, strong π-π interactions were observed between the phenyl rings attached to the triazine ring of the L1 ligand and the triazine ring of adjacent molecules in the crystal lattice. Hirshfeld analysis revealed that the hydrogen bond contribution to the surface was 13.6%, with H···H interactions making a dominant contribution, accounting for 53.3% of the surface interactions.

Acknowledgment

We thank the University of Qom for their assistance with this project.

References

[1] Ruiz-Azuara, L.; E. Bravo-Gomez, M. Copper Compounds in Cancer Chemotherapy. *Curr Med Chem* 2010, *17* (31), 3606–3615. https://doi.org/10.2174/092986710793213751 .

[2] Denoyer, D.; Clatworthy, S. A. S.; Cater, M. A. 16. Copper Complexes in Cancer Therapy. In *Metallo-Drugs: Development and Action of Anticancer Agents*; Sigel, A., Sigel, H., Freisinger, E., Sigel, R. K. O., Eds.; De Gruyter: Berlin, Boston, 2018; pp 469–506. https://doi.org/10.1515/9783110470734-022 .

[3] Krasnovskaya, O.; Naumov, A.; Guk, D.; Gorelkin, P.; Erofeev, A.; Beloglazkina, E.; Majouga, A. Copper Coordination Compounds as Biologically Active Agents. *Int J Mol Sci* 2020, *21* (11), 3965. https://doi.org/10.3390/ijms21113965 .

[4] Beaudelot, J.; Oger, S.; Peruško, S.; Phan, T.-A.; Teunens, T.; Moucheron, C.; Evano, G. Photoactive Copper Complexes: Properties and Applications. *Chem Rev* 2022, *122* (22), 16365–16609. https://doi.org/10.1021/acs.chemrev.2c00033 .

[5] Aflak, N.; Ben El Ayouchia, H.; Bahsis, L.; Anane, H.; Julve, M.; Stiriba, S.-E. Recent Advances in Copper-Based Solid Heterogeneous Catalysts for Azide–Alkyne Cycloaddition Reactions. *Int J Mol Sci* 2022, *23* (4), 2383. https://doi.org/10.3390/ijms23042383 .

[6] Chang, F.; Xiao, M.; Miao, R.; Liu, Y.; Ren, M.; Jia, Z.; Han, D.; Yuan, Y.; Bai, Z.; Yang, L. Copper-Based Catalysts for Electrochemical Carbon Dioxide Reduction to Multicarbon Products. *Electrochemical Energy Reviews* 2022, *5* (3), 4. https://doi.org/10.1007/s41918-022-00139-5 .

[7] Molinaro, C.; Martoriati, A.; Pelinski, L.; Cailliau, K. Copper Complexes as Anticancer Agents Targeting Topoisomerases I and II. *Cancers (Basel)* 2020, *12* (10), 2863. https://doi.org/10.3390/cancers12102863 .

[8] Li, J.-X.; Du, Z.-X.; Zhang, L.-L.; Liu, D.-L.; Pan, Q.-Y. Doubly Mononuclear Cocrystal and Oxalato-Bridged Binuclear Copper Compounds Containing Flexible 2-((3,5,6-Trichloropyridin-2-Yl)Oxy)Acetate Tectons: Synthesis, Crystal Analysis and Magnetic Properties. *Inorganica Chim Acta* 2020, *512*, 119890. https://doi.org/10.1016/j.ica.2020.119890 .

[9] Alter, M.; Binet, L.; Touati, N.; Lubin-Germain, N.; Le Hô, A.-S.; Mirambet, F.; Gourier, D. Photochemical Origin of the Darkening of Copper Acetate and Resinate Pigments in Historical Paintings. *Inorg Chem* 2019, *58* (19), 13115–13128. https://doi.org/10.1021/acs.inorgchem.9b02007 .

[10] Ikram, M.; Rehman, S.; Feroz, I.; Farzia; Khan, R.; Sinnokrot, M. O.; Subhan, F.; Naeem, M.; Schulzke, C. Synthesis, Spectral, Hirshfeld Surface Analysis and Biological Evaluation of a Schiff Base Copper(II) Complex: Towards a Copper(II) Based Human Anti-Glioblastoma Agent. *J Mol Struct* 2023, *1278*, 134960. https://doi.org/10.1016/j.molstruc.2023.134960 .

[11] Sarakinou, K. M.; Banti, C. N.; Hatzidimitriou, A. G.; Hadjikakou, S. K. Utilization of Metal Complexes Formed by Copper(II) Acetate or Nitrate, for the Urea Assay. *Inorganica Chim Acta* 2021, *517*, 120203. https://doi.org/10.1016/j.ica.2020.120203 .

[12] Mujahid, M.; Trendafilova, N.; Rosair, G.; Kavanagh, K.; Walsh, M.; Creaven, B. S.; Georgieva, I. Structural and Spectroscopic Study of New Copper(II) and Zinc(II) Complexes of Coumarin Oxyacetate Ligands and Determination of Their Antimicrobial Activity. *Molecules* 2023, *28* (11), 4560. https://doi.org/10.3390/molecules28114560 .

[13] SEGUEL, G. V; RIVAS, B. L.; PAREDES, C. STUDY OF THE INTERACTIONS BETWEEN COPPER(II) ACETATE MONOHYDRATE AND OROTIC ACID AND OROTATE LIGANDS. *Journal of the Chilean Chemical Society* 2010, *55* (3), 355–358. https://doi.org/10.4067/S0717-97072010000300018 .

[14] Gominho, J.; Lourenço, A.; Marques, A. V.; Pereira, H. An Extensive Study on the Chemical Diversity of Lipophilic Extractives from Eucalyptus Globulus Wood. *Phytochemistry* 2020, *180*, 112520. https://doi.org/10.1016/j.phytochem.2020.112520 .

[15] Mancia, M. D.; Reid, M. E.; DuBose, E. S.; Campbell, J. A.; Jackson, K. M. Qualitative Identification of Dibenzoylmethane in Licorice Root (*Glycyrrhiza Glabra*) Using Gas Chromatography-Triple Quadrupole Mass Spectrometry. *Nat Prod Commun* 2014, *9* (1), 1934578X1400900. https://doi.org/10.1177/1934578X1400900127 .

[16] Li, S. Chemical Composition and Product Quality Control of Turmeric (Curcuma Longa L.). *Pharm Crop* 2011, *5* (1), 28–54. https://doi.org/10.2174/2210290601102010028 .

[17] Amalraj, A.; Pius, A.; Gopi, S.; Gopi, S. Biological Activities of Curcuminoids, Other Biomolecules from Turmeric and Their Derivatives – A Review. *J Tradit Complement*

Med 2017, *7* (2), 205–233. https://doi.org/10.1016/j.jtcme.2016.05.005 .

[18] Slika, L.; Patra, D. Traditional Uses, Therapeutic Effects and Recent Advances of Curcumin: A Mini-Review. *Mini-Reviews in Medicinal Chemistry* 2020, *20* (12), 1072–1082. https://doi.org/10.2174/1389557520666200414161316

[19] Kotha, R. R.; Luthria, D. L. Curcumin: Biological, Pharmaceutical, Nutraceutical, and Analytical Aspects. *Molecules* 2019, *24* (16), 2930. https://doi.org/10.3390/molecules24162930 .

[20] Chiyindiko, E.; Malan, F. P.; Langner, E. H. G.; Conradie, J. Conformational Study of [Cu(CF3COCHCO(C4H3X))2] (X = O or S), a Combined Experimental and DFT Study. *J Mol Struct* 2019, *1198*, 126916. https://doi.org/10.1016/j.molstruc.2019.126916 .

[21] Chiyindiko, E.; Stuurman, N. F.; Langner, E. H. G.; Conradie, J. Electrochemical Behaviour of Bis(β-Diketonato)Copper(II) Complexes Containing γ-Substituted β-Diketones. *Journal of Electroanalytical Chemistry* 2020, *860*, 113929. https://doi.org/10.1016/j.jelechem.2020.113929 .

[22] Xu, D. F.; Shen, Z. H.; Shi, Y.; He, Q.; Xia, Q. C. Synthesis, Characterization, Crystal Structure, and Biological Activity of the Copper Complex. *Russian Journal of Coordination Chemistry* 2010, *36* (6), 458–462. https://doi.org/10.1134/S1070328410060060 .

[23] Radzyminska-Lenarcik, E.; Witt, K. Solvent Extraction of Copper Ions by 3-Substituted Derivatives of β-Diketones. *Sep Sci Technol* 2018, *53* (8), 1223–1229. https://doi.org/10.1080/01496395.2017.1329838 .

[24] Valdéz-Camacho, J. R.; Ramírez-Solís, A.; Escalante, J.; Ruiz-Azuara, L.; Hô, M. Theoretical Determination of Half-Wave Potentials for Phenanthroline-, Bipyridine-, Acetylacetonate-, and Glycinate-Containing Copper (II) Complexes. *J Mol Model* 2020, *26* (7), 191. https://doi.org/10.1007/s00894-020-04453-x .

[25] Keller, M.; Ianchuk, M.; Ladeira, S.; Taillefer, M.; Caminade, A.-M.; Majoral, J.-P.; Ouali, A. Synthesis of Dendritic β-Diketones and Their Application in Copper-Catalyzed Diaryl Ether Formation. *European J Org Chem* 2012, *2012* (5), 1056–1062. https://doi.org/10.1002/ejoc.201101521 .

[26] Larson, A. T.; Crossman, A. S.; Krajewski, S. M.; Marshak, M. P. Copper(II) as a Platform for Probing the Steric Demand of Bulky β-Diketonates. *Inorg Chem* 2020, *59* (1), 423–432. https://doi.org/10.1021/acs.inorgchem.9b02721 .

[27] Spackman, P. R.; Turner, M. J.; McKinnon, J. J.; Wolff, S. K.; Grimwood, D. J.; Jayatilaka, D.; Spackman, M. A. *CrystalExplorer* : A Program for Hirshfeld Surface Analysis, Visualization and Quantitative Analysis of Molecular Crystals. *J Appl Crystallogr* 2021, *54* (3), 1006–1011. https://doi.org/10.1107/S1600576721002910 .

[28] McKinnon, J. J.; Jayatilaka, D.; Spackman, M. A. Towards Quantitative Analysis of Intermolecular Interactions with Hirshfeld Surfaces. *Chemical Communications* 2007, No. 37, 3814. https://doi.org/10.1039/b704980c .